

Comparative analysis of ESC and Flight Controller Communication Protocols and their impact on brushless motor response and drone control

Vitor Garcia Ribeiro*, André Carmona Hernandes†, Guilherme Barros Villela‡ and Marcelo Becker§
 Universidade de São Paulo, São Carlos, Brazil, and Universidade Federal de São Carlos, São Carlos, Brazil

ABSTRACT

This study explores the impact of communication protocols, specifically PWM and OneShot 125, between flight controllers and electronic speed controllers (ESCs) on brushless motor response and drone control. The experimental setup includes a test bench equipped with BLHeli-S ESCs and an STM32-based flight controller programmed with proportional control. Experiments quantified response time and control precision under different protocols. Data on bench angle and motor throttle were analysed using computational tools such as MATLAB. Notably, the results reveal no significant advantage in changing communication protocols. Instead, effectiveness and responsiveness are determined much more by the control loop frequency than by the rate of different protocols.

1 INTRODUCTION

In recent years, unmanned aerial vehicles (UAVs), commonly known as drones, have driven research and development of new technologies aimed at improving their efficiency and performance [1]. Among these technologies, the advancement of communication protocols is significant, promising to enhance the speed, reliability, and precision in the transmission of critical data [2].

However, to the best of our knowledge, the communication between two crucial components for the precise control of these aerial devices, the electronic speed controller (ESC) and flight controller, remains an underexplored topic in academia, often limited to user manuals and hobbyists. The current literature lacks analyses that evaluate the isolated impact of different communication protocols on the performance of drone control.

This paper aims to address this gap by conducting a comparative analysis of the response of an experimental setup subjected to two communication protocols: Standard PWM

and OneShot125, while keeping all other parameters constant. To achieve this, a test bench configured to simulate the angular control of a drone under disturbances was used. This decision was made due to the fact it can perform tests with the same set-up for a long period of time, thereby enhancing the overall protocol effect comparison. Therefore, this study aims to provide insights of the communication protocol isolated from control loop rate.

The paper has been divided into 5 parts: the first being this introduction, which provides the context and motivation for the study. The second one is concerned with the theoretical background. It will define the basis of our work, where the fundamental concepts will be introduced. The methodology used is detailed in the third section, including the experimental procedures and tools used. The fourth part focuses on the results and analysis, it will compare the theoretical assessment developed with the results achieved. The last part is the conclusion, where we will summarize the findings, discuss their implications, and suggest potential directions for future research.

2 THEORETICAL BACKGROUND

In this section, we address our problem in two main areas: an overview of Electronic Speed Controllers (ESCs), their firmware, and the communication protocols they use to interact with flight controllers, and a mathematical derivation to support further analysis.

2.1 ESCs and Firmware

Electronic Speed Controllers (ESCs) are essential components in the operation of UAVs, particularly in multicopter configurations such as drones. They are responsible for regulating the speed and direction of brushless motors, which they achieve by receiving control signals from the flight controller and modulating the power supplied to the motors [3]. The ESC interprets these signals and adjusts the motor speed accordingly, ensuring stable flight dynamics and manoeuvrability.

Modern ESCs come with various firmware options, among which BLHeli-S stands out due to its advanced features and ease of customization [4, 5]. This firmware provides improved throttle response, reduced noise, and enhanced compatibility with different communication protocols [6]. These attributes make BLHeli-S particularly suitable for

*E-mail: v.ribeiro@usp.br

†E-mail: andre.hernandes@ufscar.br

‡E-mail: villela.guilherme@usp.br

§E-mail: becker@sc.usp.br

research that requires consistent and reliable motor control, as in the present study.

2.2 Communication Protocols

The communication between the flight controller and the ESCs is facilitated by several protocols, each with distinct characteristics. For this study, we focus on two protocols: Pulse Width Modulation (PWM) and OneShot125.

These protocols were selected due to their simplicity and relevance in practical applications, providing a focused and cautious approach to this relatively uncharted topic.

Standard PWM is one of the most traditional methods for communicating between a flight controller and an ESC [7]. It operates by sending a series of pulse signals at 20 ms rate, where the width of each pulse corresponds to a specific throttle position or motor speed. Typically, standard PWM signals range from 1 ms (minimum throttle) to 2 ms (maximum throttle) [8]. The main advantage of PWM is its simplicity, making it compatible with almost all ESCs and flight controllers [4]. However, the relatively slow update rate can introduce latency, which might affect the responsiveness of the drone's control system [8, 4, 9].

OneShot125 is a more recent protocol than PWM, designed to overcome some of its limitations. It reduces the pulse width to a range of 125 μ s to 250 μ s, significantly increasing the signal update rate [9]. OneShot125 also reduces the latency introduced by the control loop, theoretically enhancing the overall performance of the drone. However, the increased complexity and the need for compatible hardware can be considered as potential drawbacks.

By analysing these two protocols, this study aims to empirically evaluate these theoretical advantages and limitations.

2.3 Mathematical derivation

Given the aforementioned problem, we now derive a mathematical model to aid our analysis. This model will be derived using concentrated parameters, as a way to encapsulate dominant effects. It is focused on a test bench (Figure 1) previously constructed and validated in a prior academic work [10].

First, some hypotheses must be drawn:

1. The dominant poles of a brushless DC motor can be modelled as a simple brushed DC motor [11].
2. A bearing damping is significant and must be included in the analysis of the motor equation.
3. The damping term in the bench equation consolidates all velocity-related losses, including both bearing losses and aerodynamic drag on the rod.
4. Changes in thrust due to propeller movement are not considered significant. This is because their effects can be approximated by the damping term mentioned in hypothesis (3), thus not requiring separate consideration.

5. The thrust constant and torque/power constant of the propeller are assumed constant and independent of the Reynolds number. Although it appears that it may not hold, experimental tests on some propellers, in special the ones used (GWS 5"x3"), show that a constant term can be used [12].
6. For the tests in consideration, the air density is constant.
7. By using disturbance analysis, the term $\Delta\omega^2$ may be neglected. This assumption is based on the premise that the variations in angular velocity squared are minor and do not significantly impact the overall system dynamics.
8. The angular sensor has an antialiasing first-order low-pass filter with bandwidth at 13 Hz.

From these hypotheses, it can be derived that:

$$\dot{\omega} = \frac{K_\tau \cdot V_{dc}}{R \cdot J_m} \cdot u - \left(\frac{K_\tau \cdot K_\omega}{R \cdot J_m} + \frac{B_m}{J_m} \right) \cdot \omega - \frac{d}{J_m} \cdot \omega^2 \quad (1)$$

In which $\dot{\omega}$ is the rotor angular acceleration, ω is the rotor speed, K_τ and K_ω are the torque and speed constants of a dc motor, V_{dc} is the nominal supply voltage, u is the control action, in the $[0, 1]$ domain, J_m is the rotor plus propeller inertia, R is the dc motor resistance, B_m is the bearing damping and d is the consolidation of $\frac{1}{2} \cdot \rho \cdot C_Q \cdot A \cdot R_p^3$, which is the aerodynamic drag generated by the propeller.

It is worth mentioning that ρ is the air density, A is the propeller disk area, C_Q is the torque constant and R_p is the propeller radius.

By applying disturbance analysis on equation 1, we achieve:

$$\Delta\dot{\omega} = \frac{K_\tau \cdot V_{dc}}{R \cdot J_m} \cdot \Delta u - \left(\frac{K_\tau \cdot K_\omega}{R \cdot J_m} + \frac{B_m}{J_m} + \frac{2d\omega_H}{J_m} \right) \cdot \Delta\omega \quad (2)$$

where $\Delta\omega$ is the disturbed speed, Δu , disturbed control action, u_H the control action to achieve hover condition and ω_H the rotor speed in hover condition.

Equation 2 is easily solved and has the form presented in equation 3.

$$\Delta\omega = \frac{K_\tau \cdot V_{dc} \cdot \Delta u}{R \cdot J_m \cdot p} (1 - e^{-pt}) \quad (3)$$

with $p = \left(\frac{K_\tau \cdot K_\omega}{R \cdot J_m} + \frac{B_m}{J_m} + \frac{2d\omega_H}{J_m} \right)$. However, this assumes an instantaneous response given a change in control action, so we can extend equation 3 by including a time delay due to the communication protocol:

$$\Delta\omega = \frac{K_\tau \cdot V_{dc} \cdot \Delta u}{R \cdot J_m \cdot p} (1 - e^{-p(t-a)}) \quad (4)$$

in which a represents the included delay.

We may also look on how the current should behave, by applying the result from equation 4 to the dc motor model, we achieve:

$$K'(1 - c_1 \cdot e^{-p(t-a)})\Delta u = \Delta i \quad (5)$$

in which K' and c_1 will be constants derived from equation 4. As one may observe, the current behaviour follows a typical first-order system.

If we extend our analysis to the whole bench, as described in equations 6 and 7 we are left with:

$$T = \frac{1}{2} \cdot \rho \cdot C_T \cdot A \cdot R_p^2 \cdot \omega^2 \quad (6)$$

$$\ddot{\theta} = \frac{\ell \cdot (T_f - T_r) - B \cdot \dot{\theta}}{J} \quad (7)$$

Equation 6 relates the angular velocity of the propellers to the thrust force T they generate, where C_T is the thrust coefficient.

As for equation 7, it describes the angular acceleration of the rod, influenced by the difference in thrust between the front and rear propellers, where ℓ is the distance from the centre of the motor, B is the overall drag, J is the overall inertia and θ is the angle position of the rod in the test bench.

With a little bit of effort on algebra arrangement, combining the equations 2, 6 and 7, adding the sensor effect on the plant, and doing the z-transform, one may see the overall plant discretized as described by equation 8.

$$\frac{\Delta\omega}{\Delta U}(z) = \frac{A_1 z^4 + A_2 z^3 + A_3 z^2 + A_4 z + A_5}{(z-1)(z - e^{-\frac{B_m T}{J_m}})(z - e^{-pT})(z - e^{-T/\tau})} \quad (8)$$

Where T is the sampling time given by the control loop rate and $1/\tau$ is the sensor bandwidth. By renaming the poles, for simplicity's sake, we now may add the delay effect, that follows equation 9:

$$\frac{\Delta\omega}{\Delta U}(z) = \frac{(A_1 z^4 + A_2 z^3 + A_3 z^2 + A_4 z + A_5)(z - zd)}{z^2(z-1)(z-p_1)(z-p_2)(z-p_3)} \quad (9)$$

It can be seen that the delay factor changes the plant order and adds a zero, given that the delay is bigger than one control loop. Also, it is possible to see that a comparison with the same control loop rate is paramount given that the sampling time changes the poles values, and thus, changes the behaviour of the bench.

3 METHODOLOGY

3.1 Experimental Setup

For the experiments, a proprietary test bench (Figure 1) was used.

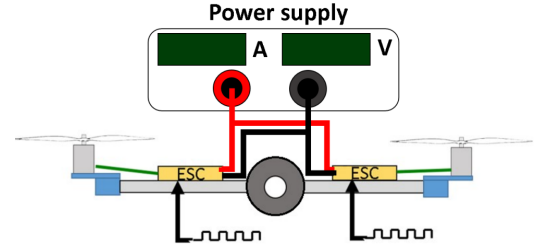


Figure 1: Test bench schematic [10]

The test bench includes a rigid aluminium rod balanced at its centre and connected to the device via a freely rotating axis supported by two bearings fixed to the base. At each end of the rod, brushless motors with attached propellers are mounted, and two BLHeli-S 30 A ESCs are fixed along the rod to control the motors.

At the centre of the structure is the power distribution system and a flight controller, based on the STM32F401 microcontroller. The STM connects via serial connection with a computer, to storage the data read.

A potentiometer serves as the primary sensor for angle measurement. The potentiometer is calibrated to provide a direct reading of the angular displacement, with the reference angle set at 0 degrees, which corresponds to the equilibrium position where the rod is parallel to the horizontal plane. Additionally, it has a low pass filter aimed at reducing noise from the power supply. This setup allows for precise assessment of the system's dynamic behaviour.

Lastly, the power supply is provided by a switched-mode power supply that provides continuous current to all components.

3.2 Motor current measurement

To attest any delay between the change in control action and the change in motor speed, it was initially inserted a 0.66 Ω - 50 W resistor in series with one of the motors. As a result, it was possible to measure the current flow on the motor.

As described by equation 5, a step disturbance on the controller is expected to result in the disturbed current following a first-order step response curve. Therefore, the proposed experiment involved activating both motors at the same speed (using 40% control action). After 6 seconds, to ensure steady-state conditions were achieved, the controller loop is initiated, using 50% control action as the hover condition.

When the loop starts, at the beginning of the control signal, a LED is toggled on each control step. This enables the measurement of the delay between the change in control action until the current first-order curve starts, marking when the motor received the command.

3.3 Controller Configuration

The controller used in this study employs a simple proportional control mechanism to maintain the desired angular

position of the test bench. It is effective enough for simple systems like this, eventually reaching a steady state without errors. A non PID approach was chosen to try highlighting the differences in control action under the different protocols, rather than using a more robust and generally faster PID controller. It is also worth mentioning that the same control rate (100 Hz) was chosen in all experiments.

The proportional controller operates with a gain value of $K_p = 60$, applied to the angular error measured in radians. Following that, the overall control action is divided in half. For the right motor, a hover value is added, and for the left, the hover value is subtracted from the split control action, thus, creating a correctional torque on the bench. The hover value used was 50% of the control action. This approach ensures that the control actions are symmetric and achieves the stability of the test bench.

Expressed in PWM units, the control signals have a resolution of 500 steps. This high resolution allows for fine adjustments to the motor speeds, with each step corresponding to a 0.2% change in the PWM signal. This resolution enables a precise control for maintaining the desired angular position and minimizing late oscillations.

3.4 Experimental Procedures

All experiments are conducted using a computer connected to the flight controller via a USB cable. A serial console application, such as PuTTY, is employed to communicate with the flight controller and to initiate one of the four pre-programmed¹ routines: two for calibrating the communication protocols and two for starting the stabilization procedure, which includes the proportional controller described in the section 3.3.

An experimental run begins with the initialization of the test bench, ensuring that all components are securely mounted and properly connected. Then, the rod is tilted to its maximum permissible angle (approximately 50 degrees from reference) to ensure the same starting point for all trials, given it has a physical barrier. Using the serial commands, we either choose calibration of PWM or OneShot when the change in protocol is needed, or simply run PWM or OneShot, depending on the run number.

The successful identification of the protocol by the ESC is confirmed through auditory signals (beeps) [6].

To ensure a smooth transition between initialization and the controller phase, an intermediate step is needed. Before the controller is activated, both motors are set to run at 40% power for 6 seconds to stabilize the rotor speed. Following this, a control stage consisting of 400 points is executed over 4 seconds at a frequency of 100 Hz.

To ensure data reliability and validity, 28 repetitions were done for each protocol, totalizing 56 runs. The order of experiments with the protocols were randomized. This was chosen because repetition reduces outlier impact and, by randomiz-

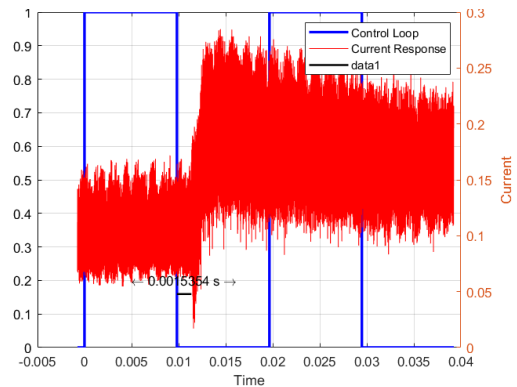
ing the protocols, it prevents drift to affecting one protocol or another [13].

4 RESULTS AND DISCUSSION

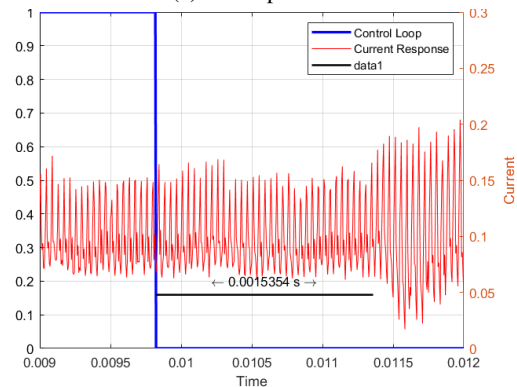
4.1 Delay and Current Analysis

After completing the experiments described earlier, the results underscore one difference between the protocols. Figure 2a illustrates the variation in current as a function of the control loop for the tests under the PWM protocol. For a more granular analysis, particularly to determine the response delay time, Figure 2b provides a detailed view. The same applies for the OneShot125 protocol, as depicted in Figure 3.

In these graphs, it is possible to roughly identify the first-order behaviour assumed previously.



(a) PWM protocol

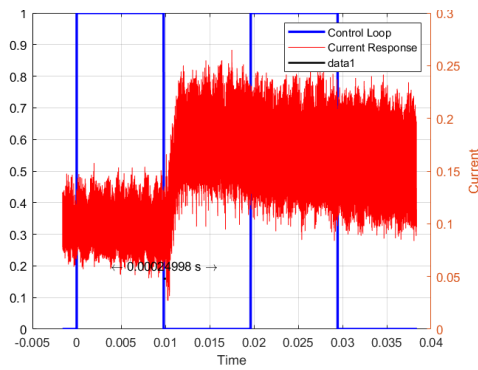


(b) PWM protocol in detail

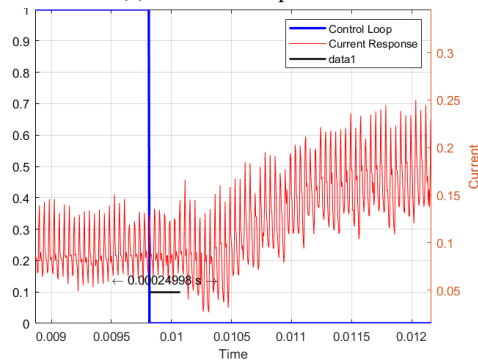
Figure 2: PWM detected delay

Through careful examination, the delay in the PWM signal was approximately identified as being about 11.5 milliseconds after the first control loop, while for OneShot125, the delay is 10.25 milliseconds. Therefore, our experiments shown that different protocols have different delay responses.

¹The program code can be found in Appendix A:



(a) OneShot125 protocol



(b) OneShot125 protocol in detail

Figure 3: OneShot125 detected delay

Moreover, the delays perceived can be divided in two parts, one equal to the control loop rate, given that our signal implementation only updated the duty cycle on the next loop, and the other part, dependent on the protocol used. The delay phenomenon was modelled at equation 9.

4.2 Comparative Analysis of Protocols

In this section, we present the findings from the experiments conducted using the test bench setup. Figure 4 shows the consolidation of all 56 runs performed with both protocols. It starts the moment the controller is activated. The solid lines demonstrate the calculated mean of experiments, and the coloured region the standard deviation range.

From a preliminary analysis of the data, several observations can be made. First, there are about 400 milliseconds before the motors can outrun the counter torque and start tilting the rod - the primary hypothesis is a mass unbalance between both arms in the rod. Subsequently, the rod achieves a dynamic behaviour typical of a second-order underdamped system, stabilizing after a few seconds (not contained in this graph). This can be easily traced given a pole at the integrator position and the mechanical pole given by $e^{-B_m T/J_m}$.

It also appears that there is a small difference between both protocols, however because of the variability between trials, a statistical analysis is required to state it or not.

The error accumulated over time, arising from factors

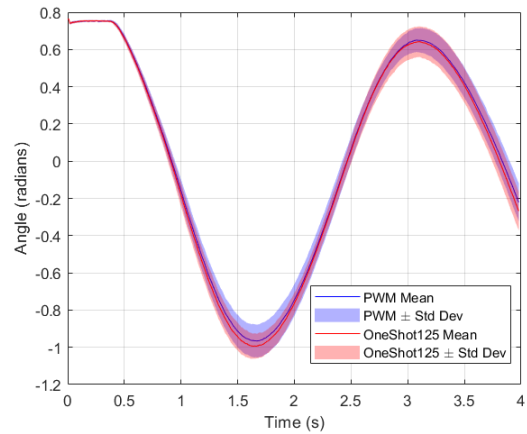


Figure 4: Mean angle of all runs with standard deviation ranges

such as control action rounding, angle measurements inaccuracies, dissipative aerodynamic effects, and other disturbances, poses a challenge for the comparative analysis between the two protocols. This is because a sudden surge in error at any given moment alters the system’s response, which in turn affects subsequent readings and further modifies the control actions and overall system behaviour. This cumulative nature introduces a growing divergence between the system’s expected and actual responses, which can mask the true effects of the communication protocols under study. As time progresses, these discrepancies become more pronounced, leading to an increase in the standard deviation between experimental runs, as observed in Figure 5.

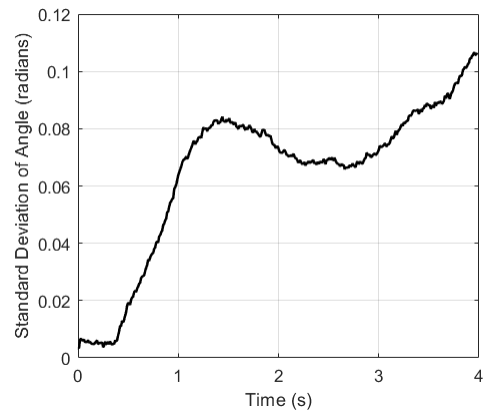


Figure 5: Standard deviation of the experimental data

Consequently, the longer the experiments run, the more difficult it becomes to attribute differences in system response solely to the communication protocol rather than to accumulating errors. This phenomenon suggests that the validity of the experiment, from a statistical perspective, is more reliable

http://www.imavs.org/

when focusing on the initial moments, where the accumulated error remains relatively small and controlled. This is one of the reasons it was decided to sample only 4 seconds of data. By limiting the analysis to this early phase, the intrinsic effects of the communication protocols are more accurately isolated, ensuring a more precise comparison of their performance without the confounding influence of escalating errors.

For these reasons, we focus our analysis on the rise time required to first achieve the horizontal plane and compare the two means using a Student's Two-Sample T-Test. This statistical test, given by equation 10, is particularly useful for determining whether there is a significant difference between the means of two independent samples [13, 14].

$$t = \frac{\bar{X}_1 - \bar{X}_2}{\sqrt{\frac{S_1^2}{n_1} + \frac{S_2^2}{n_2}}} \quad (10)$$

Where \bar{X}_1 and \bar{X}_2 are the observed means, S_1^2 and S_2^2 are the variances, and n_1 and n_2 are the sample size of each sample.

From the data acquired, the value of t was calculated as:

$$t = \frac{0.918 - 0.909}{\sqrt{\frac{0.0484^2}{28} + \frac{0.0515^2}{28}}} \approx 0.6738$$

This calculated t-value is far below the critical value for any reasonable confidence level, indicating that there is insufficient evidence to reject the null hypothesis [14]. In other words, the experimental results are not statistically significant to suggest any meaningful difference between the two protocols.

This conclusion holds for all points of analysis. As time progresses, the standard deviation increases, but the mean value remains close for both protocols, causing the t-value to decrease even further.

4.3 Interpretation of Results

The findings from our experiments reveal several key insights into the impact of communication protocols (PWM and OneShot125) on the system's response time and stability in a controlled test environment. Despite the initial hypothesis that OneShot125, with its faster communication rate, would result in a noticeably quicker response and more stable control compared to the standard PWM protocol, the experimental data do not support a statistically significant difference between the two, when all the other factors were held constant, and only the protocol was changed.

The delay measurements for both protocols suggest that while the OneShot125 protocol does indeed reduce communication delay (approximately 250 microseconds compared to 1.5 milliseconds for PWM), this difference does not translate into a significantly different overall system performance in the control plant developed for the present work.

Overall, as observed by equation 9, the delay part introduced by solely the protocol behaviour, apart from the 10 ms

given next cycle update (which introduces a pole in zero), creates a pole in zero and a zero on the left of that pole, which has quick decay over time. Given that, it can be seen that our platform presents two dominant poles, one at $z = 1$, and integrator, and the other at $z = e^{-\frac{B_m T}{J_m}}$, which represents the overall mechanical pole from the rod, and, as one may see by pure inspection, the controlled (damped) frequency has a value of more or less 0.6 Hz ($\approx 1.5s$), and it is way more dominant than the delay effect.

Therefore, for slower systems where these dominant poles are near the integrator pole, the impact of communication delays is negligible. However, in cases where the mechanical poles are closer to the 0 pole, such as in high-performance applications like racing drones, these delays could become more consequential. Again, analysing Equation 9 after discretization, it becomes evident that the sampling period significantly impacts the system by altering all poles. Consequently, switching to a faster protocol, such as OneShot125, may be justified, as it allows for a control loop frequency of up to 1 kHz, compared to PWM, which is limited to a maximum of 250 Hz.

On a more practical note, the PWM can have a more refined range for the control action vector, since it needs 1 ms for the whole range, thus, a 0.1 microsecond timer resolution, will lead to a 0.01% step. On the other hand, to achieve the same precision with OneShot125, it will be needed a timer resolution of 12.5 nanoseconds, which corresponds to 80 MHz, thus, a minor change in frequency may induce a control action error.

4.4 Implications and Future Directions

The overall results suggest that the choice of the communication protocol should consider two aspects, the first one is the control loop rate, which should be guided by the dominant poles of the drone, and the other aspect should be control action resolution. Therefore, if the control engineer, given robustness, parametric variation, noise immunity decides that the drone may be controlled by a frequency less than 250 Hz (4 ms), the PWM may be chosen, given that the introduced delay does not interact with the dominant poles. This decision would favour the control resolution and a healthier hardware communication, and, as showed in our experiments, there is no difference compared to the OneShot protocol. On the other hand, if the control engineer decides it needs to be controlled with higher frequencies, one may decide to use the OneShot protocol.

Future research should consider extending the analysis to more complex operational conditions, including high-performance controllers, that are immune to disturbances, noise and parametric variations. Such controllers may need to affect higher frequencies and thus, the protocol delays may be a contributing factor. Additionally, investigating the impact of the communication protocol on other aspects of performance, such as energy efficiency or robustness to noise,

could provide a more comprehensive understanding of their role in UAV systems.

Based on the findings of this study, it can be suggested that the assembly and component selection for an aerial vehicle should not overly prioritize the choice of communication protocol between ESCs, motors, and flight controllers. Likewise, the selection of hardware should not be limited solely to ensure compatibility with "modern" protocols. Instead, other factors should also be considered beyond the protocol's update rate. These include the availability of protocol-specific technologies that offer distinct advantages — such as telemetry feedback, regenerative braking, or active freewheeling, available in some protocols — as well as the capability (and necessity) to implement a more frequent control loop. Furthermore, considerations like the cost and efficiency of the hardware are even crucial and should only be impacted by the protocol's update rate if the application demands extremely response time and the system is very responsive - although it still needs to be confirmed by future research.

5 CONCLUSION

This study presents a comparative analysis of two communication protocols, PWM and OneShot125, and their impact on brushless motor response and drone control.

Different delays were detected between the protocols, with OneShot125 showing faster responsiveness. However, for the specific case of our experimental setup, the small communication delays have not shown significantly effect in the overall dynamics. Thus, the small improvements of OneShot125's reduced latency do not manifest in a substantial way under these test conditions. While the delays were detected and measured, their effect on most real-world performance is expected to be minimal. This conclusion is particularly valid for larger, slower drones, where such delays do not introduce noticeable differences. However, for smaller, faster, or more aggressive drones, these delays might have a more pronounced impact, requiring further exploration.

With the methodology hereby presented, we hope to enable future work to be carried out, with a focus on enhancing our understanding of existing protocols in different applications. Consequently, it will be possible to guide better decisions regarding practical UAV applications.

ACKNOWLEDGEMENTS

This work was supported by National Council for Development and Research (CNPQ), Brazil, grant no. 2023-1263, and by São Paulo Research Foundation (FAPESP) grant no. 2023/11661-0.

REFERENCES

- [1] Syed Agha Hassnain Mohsan, Nawaf Qasem Hamood Othman, Yanlong Li, Mohammed H. Alsharif, and Muhammad Asghar Khan. Unmanned aerial vehicles (uavs): practical aspects, applications, open challenges, security issues, and future trends. *Intelligent Service Robotics*, January 2023.
- [2] Drago Hercog. *Communication Protocols: Principles, Methods and Specifications*. Springer International Publishing, 2020.
- [3] H. V. Rahul, R. Rachana, L. G. Vaishnavi, V. Nesara, G. K. Savyasachi, and Alfred Vivek D'Souza. Electronic speed controllers: A review. *International Journal of Engineering Research & Technology (IJERT)*, 10(11), 2022. ICEI – 2022.
- [4] Oscar Liang. Overview of ESC Firmware and Protocols: How Flight Controllers and ESCs Communicate. <https://oscarliang.com/esc-firmware-protocols/>, nov 2023. Accessed: 2024-06-03.
- [5] ArduPilot Dev Team. BLHeli32 and BLHeli-S. <https://ardupilot.org/copter/docs/common-blheli32-passthru.html>, 2024. Accessed: 2024-05-20.
- [6] SiLabs. *Operation manual for BLHeli*. TME, Available at <https://www.tme.eu/Document/565a6d126189bb1b31b17819c38dcc5c/Bullet%20firmware%20instruction.pdf>, 2023. Accessed: 2024-05-12.
- [7] Kristen N. Mogensen. Motor-control considerations for electronic speed control in drones. *Analog Applications Journal*, 4Q 2016:1–6, 2016.
- [8] Jian Sun. *Pulse-Width Modulation*, pages 25–61. Springer, London, 2012.
- [9] A.L. Imoize, S.M.N. Islam, T. Poongodi, L.K. Ramasamy, and B.V.V.S. Prasad. *Unmanned Aerial Vehicle Cellular Communications*. Unmanned System Technologies. Springer International Publishing, 2022.
- [10] Vitor Campos and André Carmona Hernandez. Educational testbed for aerial angular control: Project and study case. In *LARS/SBR/WRE*, pages 522–527, 2018.
- [11] Mark Cutler and Jonathan P How. Analysis and control of a variable-pitch quadrotor for agile flight. *Journal of Dynamic Systems, Measurement, and Control*, 137(10):101002, 2015.
- [12] Robert W Deters. *Performance and slipstream characteristics of small-scale propellers at low Reynolds numbers*. University of Illinois at Urbana-Champaign, 2014.
- [13] Nist/Sematech. *Handbook of Statistical Methods*. <https://doi.org/10.18434/M32189>, 2012.
- [14] George Casella and Roger Berger. *Statistical inference*. CRC Press, 2024.

APPENDIX A: RESOURCES

All relevant codes used in this project will be available in a GitHub repository at: <https://github.com/VitorGaRi/BenchTestProtocolsComparison>.